J Therm Anal Calorim (2017) 127:697–708
DOI 10.1007/s10973-016-5515-6

Thermal behaviour of some novel biologically active complexes with a triazolopyrimidine pharmacophore

Larisa Calu[1,2] · Mihaela Badea[1] · Romana Cerc Korošec[3] · Peter Bukovec[3] · Constantin G. Daniliuc[4] · Mariana Carmen Chifiriuc[5,6] · Luminiţa Măruţescu[5] · Camelia Ciulică[1] · Gina Serban[1] · Rodica Olar[1]

Received: 30 October 2015 / Accepted: 29 April 2016 / Published online: 20 May 2016

Abstract A new derivative 5-phenyl-7-methyl-1,2,4-triazolo[1,5-*a*]pyrimidine (pmtp) was synthesised by [1 + 1] condensation of benzoylacetone and 3-amino-4H-1,2,4-triazole. Single crystal X-ray diffraction revealed that the pmtp crystallises in monoclinic system, P21/n spatial group. In order to modulate the biological activity, new species M(pmtp)Cl_2·nH_2O (M: Co, $n = 2$; M: Ni, $n = 3$; M: Cu, $n = 1$; M: Zn, $n = 0$) were synthesised by one-pot method. Chemical analysis, molar conductivities, IR, UV–Vis-NIR and EPR spectroscopy, as well as magnetic data recorded at room temperature provided useful information concerning the molecular formula, stereochemistry and ligand coordination mode. The modifications at heating and also the thermodynamic effects that accompany them were investigated by thermal analysis. The nature of the gaseous products formed in each step was evidenced by simultaneous TG/DSC/EGA measurements. Processes as water and chloride elimination, fragmentation and oxidative degradation of the triazolopyrimidine derivative were observed during the thermal studies. The final residue was the most stable metallic oxide as X-ray powder diffraction indicates. Zinc (II) and copper (II) complexes exhibited the most significant antimicrobial activity against a wide spectrum of Gram-positive and Gram-negative bacterial strains, both reference and clinical resistant ones, in planktonic and biofilm state. The minimal biofilm eradication values were two to four times lower than the minimal inhibitory concentrations demonstrating the potential of the obtained complexes to act as anti-pathogenic agents.

Keywords Antimicrobial activity · Complex · 5-phenyl-7-methyl-1,2,4-triazolo[1,5-*a*]pyrimidine · One-pot condensation · Thermal behaviour

This work was partially supported by University of Bucharest.

Electronic supplementary material The online version of this article (doi:10.1007/s10973-016-5515-6) contains supplementary material, which is available to authorized users.

✉ Rodica Olar
rodica_m_olar@yahoo.com

[1] Department of Inorganic Chemistry, Faculty of Chemistry, University of Bucharest, 90-92 Panduri Str., 050663 Bucharest, Romania

[2] Cellular Dynamics and Flow Cytometry Department, National Institute R&D for Biological Sciences, 296 Splaiul Independentei, 060031 Bucharest, Romania

[3] Department of Inorganic Chemistry, Faculty of Chemistry and Chemical Technology, University of Ljubljana, Večna pot 113, 1000 Ljubljana, Slovenia

[4] Organisch-Chemisches Institut, Corrensstrasse 40, 48149 Münster, Germany

[5] Department of Microbiology, Faculty of Biology, University of Bucharest, 1-3 Aleea Portocalilor St., 60101 Bucharest, Romania

[6] Research Institute of the University of Bucharest, Spl. Independentei 91-95, Bucharest, Romania

Introduction

Almost all nitrogen-based heterocycles are biologically active, but triazolopyrimidine derivatives are particularly interesting having in view their similarities with purinic bases. These derivatives exhibit a large spectrum of biological activities, beginning with anti-parasitic [1], anti-inflammatory [2, 3], analgesic [2], antiviral [4], antitumor [5, 6], antimicrobial [7], and ending with cardiovascular effects [8]. From these derivatives, cevipabulin and its analogues were proved as potent anticancer agents with a

unique mechanism of action consisting in the induction of tubulin polymerisation [6]. A novel triazolopyrimidine antibiotic, essramycin was isolated from the culture broth of the marine *Streptomyces* sp. strain and proved to be active against both Gram-positive and Gram-negative bacterial strains [9]. Furthermore, some triazolopyrimidine derivatives were developed, as drugs such Trapidil, which is vasodilator acting both as platelet-derived growth factor antagonist and as phosphodiesterase inhibitor [10].

In order to modulate their biological effects, the complexation ability of triazolopyrimidine compounds was studied and allowed the generation of species with valuable antiparasitic activity [11]. Therefore, Pt(II) and Ru(III) triazolopyrimidine complexes were active on *Leishmania, Trypanosomas* and *Phytomonas* genera [12], complexes with the ligand 5-methyl-1,2,4-triazolo[1,5-*a*]pyrimidin-7(4H)-one against *Leishmania* [13], nickel complexes with a triazolopyrimidine derivative on *Leishmania infantum* and *Leishmania braziliensis* [14], triazolopyrimidine compounds containing first-row transition metals [15] and lanthanide complexes containing 5-methyl-1,2,4-triazolo[1,5-*a*]pyrimidin-7(4H)-one against *Leishmania* and *Trypanosoma cruzi* [16] and 5-methyl-1,2,4-triazolo[1,5-*a*]pyrimidin-7(4H)-one-based complexes on *Trypanosoma cruzi* [17].

Also, complexes with this class of ligands, such as a dinuclear silver compound with 5,6,7-trimethyl- [1, 2, 4] triazolo[1,5-*a*]pyrimidine with a short Ag–Ag bond [18], palladium(II) and platinum(II) organometallic complexes with 4,7-dihydro-5-methyl-7-oxo [1, 2, 4] triazolo[1,5-*a*]pyrimidine [19], platinum(IV) complexes with purine analogues [20], mono- and dinuclear platinum(II) compounds with 5,7-dimethyl-1,2,4-triazolo[1,5-*a*]pyrimidine [21], platinum(IV) coordination compounds containing 5-methyl-1,2,4-triazolo[1,5-*a*]pyrimidin-7(4H)-one as nonleaving ligand [22], hexafluoroglutarate platinum(II) complex with 5,7-dimethyl-1,2,4-triazolo[1,5-*a*]pyrimidine [23], mononuclear platinum(II) complexes with 5,7-ditert-butyl-1,2,4-triazolo[1,5-*a*]pyrimidine [24], ruthenium(III) complexes with bulky triazolopyrimidine ligands [25], dimeric ruthenium-triazolopyrimidine complex [26], ruthenium(II) and ruthenium(III) ions with 5-methyl-1,2,4-triazolo[1,5-*a*]pyrimidin-7(4H)-one [27], acetate platinum(II) compound with 5,7-ditertbutyl-1,2,4-triazolo[1,5-*a*]pyrimidine [28], organotin(IV) derivatives with 5,7-disubstituted-1,2,4-triazolo[1,5-*a*]pyrimidine [29] exhibited antitumor activity. The in vitro antitumor activity assays of Ag(I) [18], Pt(II) [19, 23, 24, 28], Pt(IV) [22], Pd(II) [19], Ru(II) [27], Ru(III) [26, 27], and Sn(IV) [29] complexes with triazolopyrimidines evidenced an antiproliferative effect against rectal, breast and bladder cancer cells. Cytotoxicity of these compounds was correlated with their stereochemistry, type of ligands, nature of pyrimidine ring substituents, as well as with their electronic and stereochemical effects. It was observed that the presence of a bulky substituent (tert-butyl or phenyl) might be an important factor in the modulation of antitumor activity [24, 28]. Concerning their antimicrobial activity, some Co(II) complexes with triazolopyrimidines exhibited good in vitro inhibitory activity against both Gram-positive and Gram-negative bacterial strains [30]. Moreover, diorganotin(IV) complexes with [1, 2, 4] triazolo-[1,5-*a*]pyrimidine derivatives were found to have promising antifungal activity [31], anti-Gram-positive bacteria [32, 33], particularly staphylococcal strains [34], both in planktonic and biofilm state.

Only one report concerning the thermal behaviour of some divalent metal ions (Co, Ni, Cu, Zn, Cd, Mn and Fe) with anionic form of 4,7-dihydro-1,2,4-triazolo-[1,5-*a*]-pyrimidine-7-one as ligand was found [35]. After water (hydration or coordination) loss, all anhydrous compounds are stable up to 350 °C, when pyrolytic decomposition starts.

In view of the pharmacological importance of triazolopyrimidines and their complexes, we report here the synthesis and characterisation of Co(II), Ni(II), Cu(II) and Zn(II) complexes with 5-phenyl-7-methyl-1,2,4-triazolo[1,5-*a*]pyrimidine, species resulted in one-pot reaction of benzoylacetone, 3-amino-4H-1,2,4-triazole and metal chloride. The ligand and complexes have been characterised by different analytical, spectral and magnetic methods. With the aim to evidence the thermal behaviour and the nature of evolved gases, these derivatives were investigated by TG/DTA and simultaneous TG/DSC coupled with the MS technique. The compounds were also screened for their antimicrobial activity against a wide range of Gram-negative and Gram-positive bacteria, as well as fungal strains.

Experimental

Materials

The high purity reagents were purchased from Sigma-Aldrich ($CoCl_2{\cdot}6H_2O$, $NiCl_2{\cdot}6H_2O$, $CuCl_2{\cdot}2H_2O$, $ZnCl_2$), Merck (benzoylacetone) and Fluka (3-amino-4H-1,2,4-triazole) and used without further purification.

Instrumentation

The content of carbon, nitrogen and hydrogen has been obtained by using a Perkin Elmer PE 2400 analyzer.

Mass spectra were recorded by electrospray ionisation tandem mass spectrometry (ESI–MS) technique operating in the positive ion mode. The sample dissolved in

acetonitrile/water (1/1) was injected directly in the Waters Micromass Quattro micro API triple quadrupole mass spectrometer with an electrospray interface.

IR spectra were recorded by using KBr pellets with a Bruker Tensor 37 spectrometer (400–4000 cm^{-1} range).

Electronic spectra were recorded by diffuse reflectance technique on a Jasco V670 spectrophotometer (200–1500 nm range, spectralon as standard).

Magnetic measurements were taken at room temperature on a Lake Shore's fully integrated Vibrating Sample Magnetometer (VSM) calibrated with $Hg[Co(NCS)_4]$.

The X-band EPR measurements were recorded with a JEOL FA100 spectrometer, and the magnetic field was calibrated with DPPH.

^1H NMR and ^{13}C NMR spectra were recorded on a Bruker Avance spectrometer (working frequency 200 MHz) at 25 °C. Chemical shifts were measured in parts per million from internal standard TMS.

The single crystal X-ray measurements were taken with a Nonius Kappa CCD diffractometer. Programs used: data collection, COLLECT [36]; data reduction Denzo-SMN [37]; absorption correction, Denzo [38]; structure solution SHELXS-97 [39]; structure refinement SHELXL-97 [40] and graphics, XP [41] (Bruker AXS, 2000), *R*-values are given for observed reflections, and wR^2 values are given for all reflections. CCDC reference number is 1433539 and contains the supplementary crystallographic data for this compound.

The simultaneous TG/DTA measurements were recorded in synthetic air atmosphere (flow rate 16.7 cm^3 min^{-1}) by using a Labsys 1200 SETARAM instrument, over the temperature range of 20–900 °C, a heating rate of 10 K min^{-1} and a sample mass of 8–30 mg.

Simultaneous thermogravimetric/dynamic scanning calorimetry/evolved gas analysis measurements (TG/DSC/EGA) were taken on a Mettler Toledo TGA/DSC1 Instrument, coupled to a Pfeiffer Vacuum ThermoStar Mass Spectrometer.

The X-ray powder diffraction patterns were collected on a PANalytical X'Pert PRO diffractometer using CuK_α radiation ($\lambda = 1.5406$ Å) in the range of 2θ from 5° to 80°.

Antimicrobial assays

The antimicrobial assays were performed on reference (bearing the ATCC code) and recently isolated clinical microbial strains, exhibiting resistance to current antibiotics recommended for testing, i.e. Gram-positive (*Staphylococcus aureus* ATCC 25923, methicillin resistant *S. aureus* - MRSA 1263, *Bacillus subtilis* ATCC 6633) and Gram-negative (*Escherichia coli* ATCC 832, *E. coli* ATCC 25922, *Klebsiella pneumoniae* 832, *K. pneumoniae* ATCC 134202, *Pseudomonas aeruginosa* ATCC 27853, *P. aeruginosa* 392) bacterial strains. The qualitative evaluation of the antimicrobial activity was performed by the adapted disc diffusion, as previously reported [42], using Mueller–Hinton Agar (MHA) medium for bacteria and Yeast Peptone Glucose (YPG) in case of fungi. The compounds were solubilised in dimethylsulfoxide (DMSO), and the starting stock solution was of 1000 μg mL^{-1} concentration.

The quantitative assay of the antimicrobial activity was performed by the liquid medium microdilution method, in 96 multi-well plates, in order to establish the minimal inhibitory concentration (MIC) and the minimal biofilm eradication concentration (MBEC) values [42]. All biological experiments were performed in triplicates.

Synthesis, analytical and spectral data for ligand and complexes

To a solution containing 1 mmol metal(II) acetate hydrated (M: Co, Ni, Cu and Zn) in 25 mL, ethanol was dropwise added a solution containing 1 mmol benzoylacetone in 10 mL ethanol and then another one formed by 1 mmol 3-amino-4H-1,2,4-triazole dissolved in 10 mL ethanol. The reaction mixture was magnetically stirred at 50 °C for 4 h, until a sparingly soluble species was formed. This product was filtered off, washed several times with cold ethanol and air-dried.

$[Co_2(pmtp)_2Cl_4(OH_2)_4]$ (**1**): Analysis found: C, 38.40; H, 3.59; N, 15.12, $Co_2C_{24}H_{28}N_8O_4Cl_4$ requires: C, 38.32; H, 3.75; N, 14.90; Yield 78 %; ESI–MS (positive mode, $CH_3CN:H_2O$ (1:1)) *m/z*: $[M + 2CH_3CN + H]^+$, 763; $[M–Cl + 2CH_3CN]^+$, 726; $[M + H]^+$, 680; $[M–CH_3]^+$, 665; $[M + H–CH_3–Cl]^+$, 631; $[1/2\ M]^+$, 340; $[M–2Cl]^{2+}$, 305; Λ_M, 9.0 Ω^{-1} cm^2 mol^{-1}.

$[Ni_2(pmtp)_2Cl_4(OH_2)_4]$ $2H_2O$ (**2**): Analysis found: C, 36.43; H, 4.02; N, 14.38, $Ni_2C_{24}H_{32}N_8O_6Cl_4$ requires: C, 36.59; H, 4.09; N, 14.22; Yield 58 %; ESI–MS (positive mode, $CH_3CN:H_2O$ (1:1)) *m/z*: $[M + H + 2CH_3CN]^+$, 763; $[M–Cl + 2CH_3CN]^+$, 726; $[M + H]^+$, 681; $[M–CH_3]^+$, 665; $[M + H–CH_3–Cl]^+$, 630; $[1/2\ M + H]^+$, 341; $[M–2Cl]^{2+}$, 304; Λ_M, 11.5 Ω^{-1} cm^2 mol^{-1}.

$[Cu_2(pmtp)_2Cl_4(OH_2)_2]$ (**3**): Analysis found: C, 39.75; H, 3.18; N, 15.62, $Cu_2C_{24}H_{24}N_8O_2Cl_4$ requires: C, 39.74; H, 3.33; N, 15.45; Yield 65 %; ESI–MS (positive mode, $CH_3CN:H_2O$ (1:1)) *m/z*: $[M + H]^+$, 690; $[M\text{-}CH_3]^+$, 674; $[M + H–CH_3–Cl]^+$, 640; $[1/2\ M + H]^+$, 346; $[M\text{-}2Cl]^{2+}$, 309; Λ_M, 8.5 Ω^{-1} cm^2 mol^{-1}.

$[Zn_2(pmtp)_2Cl_4]$ (**4**): Analysis found: C, 41.64; H, 2.82; N, 16.22, $Zn_2C_{24}H_{20}N_4Cl_4$ requires: C, 41.59; H, 2.91; N, 16.17; Yield 62 %; ESI–MS (positive mode, $CH_3CN:H_2O$ (1:1)) *m/z*: $[M + H]^+$, 694; $[M–CH_3]^+$, 678; $[M + H–CH_3–Cl]^+$, 644; $[1/2\ M + H]^+$, 348; $[M–2Cl]^{2+}$, 311; Λ_M, 13.5 Ω^{-1} cm^2 mol^{-1}.

The synthesis of 5-phenyl-7-methyl-1,2,4-triazolo[1,5-*a*]pyrimidine: To a solution containing 3.244 g (0.02 mol)

benzoylacetone in 50 mL ethanol were added 1.682 g (0.02 mol) 3-amino-4H-1,2,4-triazole and few drops of acetic acid and the reaction mixture was refluxed for 12 h until a yellow sparingly soluble product was formed. The yellow product formed was filtered off, washed several times with EtOH and recrystallised from chloroform/1-propanol (1:2, v/v). Single crystals of 5-phenyl-7-methyl-1,2,4-triazolo[1,5-*a*]pyrimidine (pmtp) suitable for X-ray diffraction were obtained from slow evaporation of a DMF/EtOH (1:1) solution. ^{1}H NMR (DMSO-d_6) δ (ppm): 2.64 (s, CH_3), 7.68 (s, CH pyrimidine), 7.72–8.30 (multiplet, Ar–H), 8.62 (s, CH triazole); ^{13}C NMR (DMSO) δ (ppm): 15.8 (C9; CH_3), 110.2 (C6; pyrimidine), 127.8, 128.8, 129.4, 131.5 (C10–C15; Ar), 146.7 (C7; pyrimidine), 155.4 (C3a; triazole), 156.3 (C2; triazole), 165.8 (C5; pyrimidine). ESI–MS (positive mode, CH_3CN) *m/z*: $[M + H]^+$, 211; $[M–CH_3]^+$, 195.

Results and discussions

Synthesis and characterisation of 5-phenyl-7-methyl-1,2,4-triazolo[1,5-*a*]pyrimidine and complexes

The one-pot reaction in 1:1:1 molar mixture of cobalt(II), nickel (II), copper (II) or zinc (II) chloride, benzoylacetone and 3-amino-4H-1,2,4-triazole produced the species $M_2(pmpt)_2Cl_4{\cdot}nH_2O$ ((**1**) M:Co, $n = 4$; (**1**) M:Ni, $n = 6$; (**3**) M:Cu, $n = 2$ and (**4**) M:Zn, $n = 0$; pmpt: 5-phenyl-7-methyl-1,2,4-triazolo[1,5-*a*]pyrimidine) (Scheme 1).

The chemical analyses are in accordance with the proposed formulas for complexes (see experimental part). The complexes behave as non-electrolytes in DMSO, the molar conductance values being very small [43].

Description of 5-phenyl-7-methyl-1,2,4-triazolo[1,5-*a*]pyrimidine structure

A summary of the crystallographic data and structure refinement for 5-phenyl-7-methyl-1,2,4-triazolo[1,5-*a*]pyrimidine (pmtp) is given at supplementary material, while the atom numbering scheme and molecular structure is provided in Fig. 1.

The compound crystallised with one independent molecule in the asymmetric unit. Dihedral angles between C7–N8–C3A, C3A–N8–N1 and N4–C3A–N3 from the fused rings are 122.3(1), 110.5(1) and 128.5(1)° as result of sp^2 hybridisation of atoms belonging to the two rings. Bonds lengths N8–C7, N8–C3A, N8–N1, N1–C2, N3–C2 range between 1.326(2) and 1.378(2) Å, and values were close to that observed for 5,7-dimethyl-1,2,4-triazolo[1,5-*a*]pyrimidine [44]. The phenyl ring is almost planar oriented compared to the triazolopyrimidine unit (θ N4–C5–C10–C11 = 5,9(2)°).

In the packing diagram, the molecules are linked into pairs through π···π staking interactions between phenyl and pyrimidine rings (shortest distance is 3.398 Å). Involving additional C-H···N contacts (C2-H2···N3 2.569 Å), a linear chain containing the corresponding dimmers is generated along the *ac*-diagonal (Fig. 2).

ESI MS, NMR and IR data

The complexes formulas were further supported by positive mode ESI mass spectrometry, which indicated as base peak corresponding to the pseudomolecular ion $[M + H]^+$ for all compounds. Moreover, other fragments that can be related to complexes dimeric structure were identified with or without chloride anions and acetonitrile molecules in components.

In the ^{1}H NMR spectrum of 5-phenyl-7-methyl-1,2,4-triazolo[1,5-*a*]pyrimidine, the signal at 2.64 ppm is assigned to methyl protons and the multiplet at 8.10 ppm is generated by phenyl ring protons. The signals of protons belonging to triazole and pyrimidine rings appear at 7.68 and 8.62 ppm, respectively. ^{13}C NMR spectrum shows the signals characteristic for triazolopyrimidine unit at 110.2, 146.7 and 165.8 ppm [13]. The carbon atom of methyl group generates a signal at 15.8 ppm and that of phenyl group are responsible for the signals noticed in the range 127.8–131.5 ppm.

The Zn(II) complex is not soluble in deuterated solvents and as results the NMR data cannot be collected.

The IR spectra of complexes (Table 1) exhibit the characteristic bands for triazolopyrimidine moiety at 1613 cm^{-1} assigned to triazolopyrimidine condensed ring (ν_{tp}) and at 1540 cm^{-1} assigned to pyrimidine ring vibration (ν_{py}), respectively [17–34]. The band corresponding to ν_{tp} vibration is shifted by 5–30 cm^{-1} to higher wavenumbers in comparison with the metal-free ligand indicating the ligand coordination through triazolopyrimidine N3 atom [17–34].

A broad band in the range 3430–3440 cm^{-1} can be assigned to ν(OH) stretching vibrations for water molecules, except for complex (**4**). Supplementary bands in the range 650–780 cm^{-1} could support the water presence as ligand in some complexes [45].

Low-intensity bands noticed in the complexes spectra in the range 450–570 cm^{-1} are an indicative of M–N and M–O coordinative bonds formation.

Electronic, EPR spectra and magnetic moments

In UV region of the electronic spectrum of ligand, three intense bands assigned to intraligand $\pi \rightarrow \pi^*$ transitions

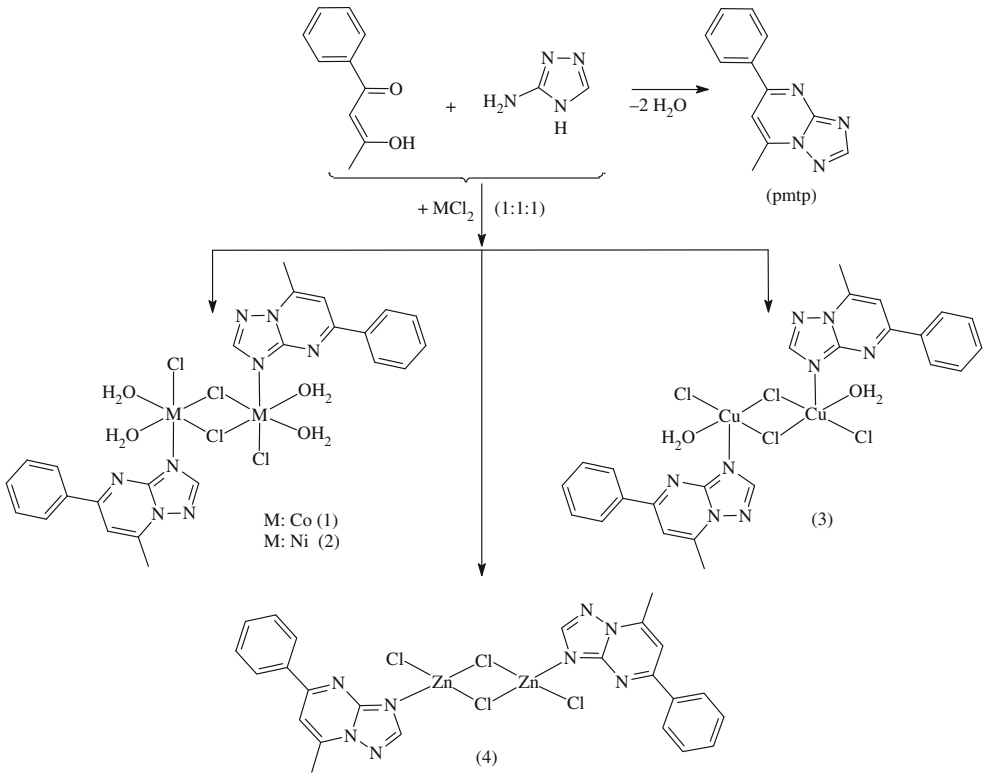

Scheme 1 Synthetic route for complexes preparation and the proposed coordination

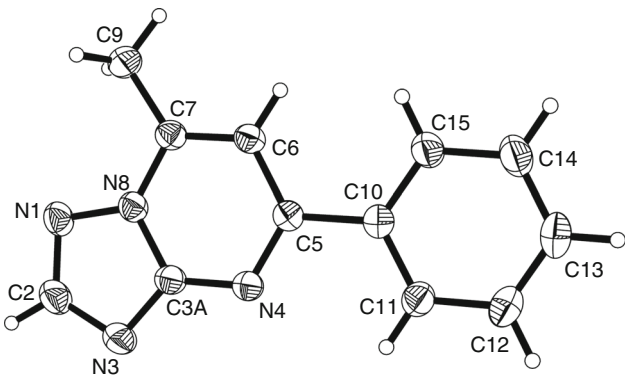

Fig. 1 The atom numbering and molecular structure of 5-phenyl-7-methyl-1,2,4-triazolo[1,5-*a*]pyrimidine (30 % probability thermal ellipsoids)

can be observed. In the complexes spectra, these bands are differently shifted as a result of coordination and interactions with the other ligands or hydration water molecules.

Three low-intensity bands appear in the electronic spectrum of compound (**1**) that can be assigned to spin allowed transitions $^4T_{1g} \rightarrow {}^4T_{2g}$, $^4T_{1g} \rightarrow {}^4A_{2g}$ and $^4T_{1g} \rightarrow {}^4T_{1g}$, in an octahedral stereochemistry (Table 2) [46]. The splitting parameter value of 8410 cm^{-1} is close to the average value for a $[Co(II)NO_2Cl_3]$ chromophore, while the nephelauxetic parameter of 0.88 is an indicative of a lower degree of covalency. The crystal field parameters (*10Dq*, *B* and β) were calculated with König's formulas [47]. The value of the magnetic moment at room temperature is also characteristic for such a stereochemistry with a T ground term and an orbital contribution as a result [48].

The broad bands that can be assigned to spin allowed transitions in an octahedral distorted geometry can be observed in electronic spectrum of Ni(II) complex as well [46]. These bands leads to a splitting parameter of 8845 cm^{-1} is according with an $[Ni(II)NO_2Cl_3]$ chromophore having a high number of donor atoms that generate a low field, such oxygen and chloride ones. A value of 0.83 for the nephelauxetic parameter indicates also a lower degree of covalency. This stereochemistry is further sustained by the room temperature magnetic moment of 3.12 B.M., as usually is observed for complexes with an A ground term [48].

The electronic spectrum of the Cu(II) complex shows the characteristic broad band with a maximum at 14,925 cm^{-1} tentatively assigned to $d_z^2 \rightarrow d_{xy}$ transition in a square pyramidal stereochemistry and a C_{2v} symmetry [46]. The value of 2.25 B.M. for the magnetic moment is characteristic for species with isolated paramagnetic centres [48].

Powder EPR spectrum of complex (**1**) exhibits a low-intensity signal with $g_{iso} = 2.119$ characteristic to a local

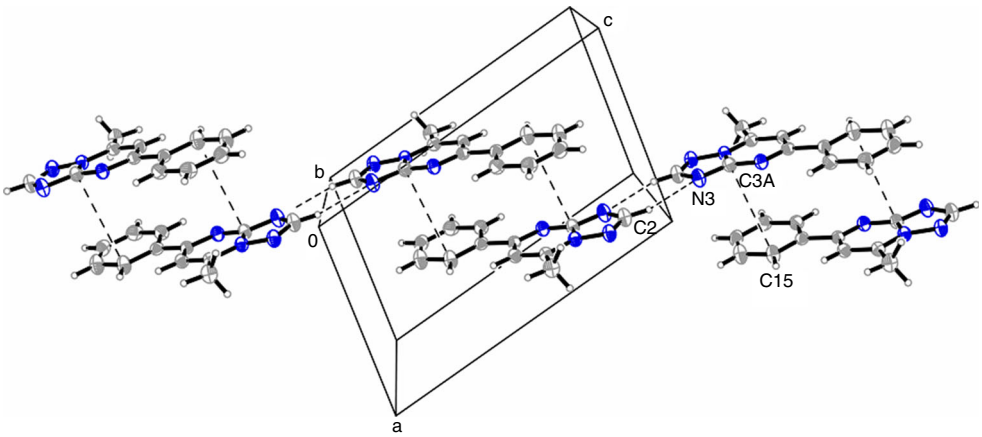

Fig. 2 Packing diagram presenting the π···π and C–H···N interactions of 5-phenyl-7-methyl-1,2,4-triazolo[1,5-*a*]pyrimidine

Table 1 IR absorption bands (cm^{-1}) for 5-phenyl-7-methyl-1,2,4-triazolo[1,5-*a*]pyrimidine and complexes

pmtp	(**1**)	(**2**)	(**3**)	(**4**)	Assignment
–	3441vs	3438s	3433m	–	$\nu(OH_2)$
3101m	3056w	3061w	3065w	3059w	$\nu(CH)$
2932w	2926w	2939w	2954w	2912w	$\nu_{as}(CH_3)$
2833w	2828w	2818w	2879w	2824w	$\nu_{s}(CH_3)$
1613s	1625s	1629s	1635vs	1617s	$\nu(C{=}N)$
1540vs	1582vs	1597s	1560vs	1544vs	
1465m	1403m	1409m	1444m	1432m	$\nu(C{=}C) + \delta_{as}(CH_3)$
1038w	1079w	1076w	1032w	1028w	$\nu(N{-}N)$
810w	843w	842w	869w	863w	$\gamma(CH)$
–	754w	772w	768w	–	$\rho_{r}(H_2O)$
–	671w	673w	656w	–	$\rho_{w}(H_2O)$
–	562w	530w	552w	500w	$\nu(M{-}N)$
–	469w	453w	478w	453w	$\nu(M{-}O)$

vs very strong, *s* strong, *m* medium, *w* weak

symmetry of copper ion lower than octahedral [49]. The aspect of the spectrum is preserved in frozen DMSO.

Thermal behaviour of ligand and complexes

The thermal behaviour of these derivatives was investigated in air by both TG/DTA and TG/DSC techniques. The results were similar and in the following the TG/DTA data will be detailed and correlated with results provided by the evolved gases analysis.

The pmtp is stable up to 192 °C and then decomposes in two steps (Fig. 3; Table 3). The endothermic effect noticed on DTA curve without mass change becomes from a phase transition such the melting is. The mass loss noticed in the first step corresponds to 51 % oxidative degradation of triazolopyrimidine derivative. The intermediate formed at 400 °C is dibenzylhydrazine according with chemical analysis and IR data. In the IR spectrum of this intermediate, the band at 3319 cm^{-1} is assigned to stretching vibration of secondary amine group, while that at 3064, 1618, 1535 and 805 cm^{-1} is associated with aromatic ring vibration modes. The methylene group was identified based on vibrations located at 2914 and 2844 cm^{-1}, respectively. This step comprises two processes according with both DTG and DTA curves. The next step results also from overlapping of several exothermic processes and corresponds with dibenzylhydrazine oxidative degradation.

The simultaneous TG/DTA curves registered for complex (**1**) are shown in Fig. 4 and indicate that complex undergoes a four steps thermal decomposition pattern. The first step consists in an endothermic elimination of water molecules up to 184 °C. The presence of ion peaks with *m/z* 18 in the MS spectra confirms this assumption, while the temperature range that corresponds to this transformation indicates the coordination nature of water molecules [50, 51]. The second step, endothermic also, corresponds to chloride anion and methyl group elimination. These decomposition processes gives rise to fragments as Cl,

Table 2 Absorption maxima, assignments and magnetic moments for ligand and complexes

Compound	Absorption maxima (cm^{-1})	Assignment	Magnetic moment (B.M.)
pmtp	38,460	$\pi \rightarrow \pi^*$	–
	29,850		
	23,255		
$[Co_2(pmtp)_2Cl_4(OH_2)_4]$ (**1**)	32,785	$\pi \rightarrow \pi^*$	4.64
	19,050	$^4T_{1g} \rightarrow {}^4T_{1g}$	
	15,750	$^4T_{1g} \rightarrow {}^4A_{2g}$	
	8365	$^4T_{1g} \rightarrow {}^4T_{2g}$	
$[Ni_2(pmtp)_2Cl_4(OH_2)_4]\cdot 2H_2O$ (**2**)	33,070	$\pi \rightarrow \pi^*$	3.12
	25,640	$^3A_{2g} \rightarrow {}^3T_{1g}$ (P)	
	15,150	$^3A_{2g} \rightarrow {}^3T_{1g}$ (F)	
	8845	$^3A_{2g} \rightarrow {}^3T_{2g}$	
$[Cu_2(pmtp)_2Cl_4(OH_2)_2]$ (**3**)	40,000, 29,410	$\pi \rightarrow \pi^*$	2.25
	14,925	$d_z^2 \rightarrow d_{xy}$	
$[Zn_2(pmtp)_2Cl_4]$ (**4**)	40,000, 31,745	$\pi \rightarrow \pi^*$	–

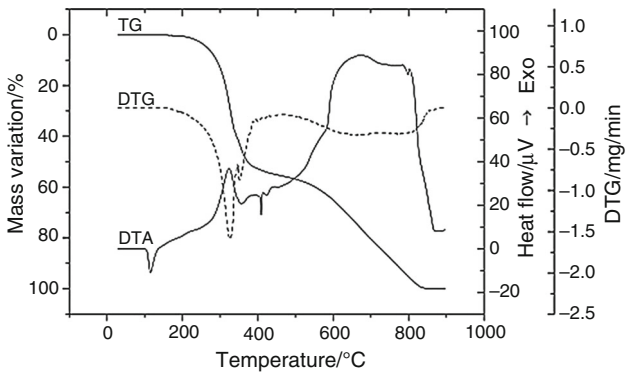

Fig. 3 TG, DTG and DTA curves of 5-phenyl-7-methyl-1,2,4-triazolo[1,5-*a*]pyrimidine (pmtp)

HCl, H_2Cl and CH_3Cl. Otherwise, such behaviour was observed for other halide complexes during thermal decomposition [52]. The decomposition continues with nitrogen containing fragments eliminations, since NO was identified along H_2O in the gaseous mixture eliminated in this step. In the next step, the rest of organic part suffers both fragmentation and oxidative degradation. Moreover, the oxidative processes predominate in this step having in view both the exothermic effects, as well as the increased quantities of CO_2, NO and NO_2 over that of nitrogen containing fragments. As result of these reactions, several exothermic processes, one of them being very strong, can be noticed on DTA curve. Also a part of cobalt(II) is oxidised at Co(III) having in view that the final product is Co_3O_4 (found/calcd. overall mass loss: 78.6/78.8 %). The nature of the final product was confirmed by powder X-ray diffraction data (ASTM 78-1970).

For compound (**2**), water molecules are eliminated in two steps and the corresponding temperature ranges indicate the nature of this species both as hydration and as coordination (Fig. 5). The chloride anions are eliminated in the second step also, considering the products with *m/z* 35 and 37 noticed in the gaseous products. The fragmentation of triazolopyrimidine moiety occurs in the same step giving rise to CH_3Cl. Moreover, the oxidation of some fragments generates products as CO_2 and NO. Two endothermic effects accompany these processes according with DTA curve. The organic ligand fragmentation proceeds with aromatic ring elimination since C_6H_5 and C_6H_4 fragments were identified by EGA. This step is not a single-process one, being an overlapping of two weak exothermic processes accordingly to the DTA curves profile. This behaviour can be the result of several reactions that occur simultaneously, such as bonds cleavage, their rearrangements, as well as aromatic moiety oxidative degradation. In the next step, the rest of organic part suffers oxidative degradation with NO, NO_2, CO_2 and H_2O as products. All these transformations finally lead to nickel (II) oxide (found/calcd. overall mass loss: 80.6/81.0 %). The nature of final product was confirmed by powder X-ray diffraction data (ASTM 78-0429).

The complex (**3**) loses the water molecules (Fig. 6) in a range that proves their coordination nature [50, 51]. Furthermore, in the MS spectra in the temperature range 50–170 °C, only fragment with *m/z* 18 can be noticed. The fragments identified in the evolved gases (Cl, NO, CH_3Cl) indicate that chloride elimination and ligand bonds cleavage together with some moieties oxidation occur in the second step. On the other hand, the small endothermic event observed on DTA curve can be the result of several

Table 3 Thermal behaviour data for 5-phenyl-7-methyl-1,2,4-triazolo[1,5-*a*] pyrimidine and complexes

Compound	Step	Thermal effect	Temperature range/°C	Δm_{exp}/%	Δm_{calc}/%	Process	Identified product by EGA or IR/powder XRD method
pmtp	1.	Endothermic	98	0	0	Melting	–
	2.	Exothermic	192–400	51.5	51.0	Oxidative degradation	dibenzylhydrazine
	3.	Exothermic	400–847	48.5	49.0	Oxidative degradation of dibenzylhydrazine	
$[Co_2(pmtp)_2Cl_4(OH_2)_4]$ (**1**)	1.	Endothermic	62–184	9.4	9.5	Water elimination	H_2O
	2.	Endothermic	184–255	22.8	22.9	Methyl and chloride elimination	CH_3Cl, Cl, HCl, H_2Cl
	3.	Endothermic	255–292	8.9	8.5	N_2H_4 fragment elimination from organic matrix	NO, H_2O
	4.	Exothermic	292–662	37.7	37.9	Oxidative degradation of organic residue and cobalt(II) partial oxidation	CO_2, H_2O, NO, NO_2, $C_2H_4N_3$, $C_2H_6N_3$
				21.2	21.2		Co_3O_4
$[Ni_2(pmtp)_2Cl_4(OH_2)_4]\cdot 2H_2O$ (**2**)	1.	Endothermic	60–130	5.0	4.6	Water elimination	H_2O
	2.	Endothermic	130–300	39.9	39.9	Water, chloride and C_3N fragment elimination from organic matrix	CH_3Cl, H_2O, Cl, H_2Cl, CO_2, NO
	3.	Exothermic	300–490	19.3	19.6	C_6H_5 fragment elimination from organic matrix	C_6H_4, C_6H_5
	4	Exothermic	490–630	16.4	16.9	Oxidative degradation of organic residue	CO_2, H_2O, NO, NO_2, CH_3Cl
				19.0	19.0		NiO
$[Cu_2(pmtp)_2Cl_4(OH_2)_2]$ (**3**)	1.	Endothermic	50–175	4.4	5.0	Water elimination	H_2O
	2.	Endothermic	175–272	26.4	26.4	Chloride and C_2N fragment elimination from organic matrix	Cl, NO, CH_3Cl
	3.	Exothermic	272–400	7.2	7.2	CN fragment elimination from organic matrix	CO_2, H_2O, NO
	4.	Exothermic	400–850	40.6	39.5	Oxidative degradation of organic residue	CO_2, HCO_2, H_2O, NO, NO_2, $C_2H_4N_3$, $C_2H_6N_3$
				21.4	21.9		CuO
$[Zn_2(pmtp)_2Cl_4]$ (**4**)	1.	Exothermic	252–341	4.5	4.6	CH_3 fragment elimination from organic matrix	CO_2, H_2O
	2.	Exothermic	341–544	15.8	15.8	Chloride elimination	Cl
	3.	Exothermic	544–787	56.2	56.1	Chloride elimination and oxidative degradation of organic residue	Cl, CO_2, HCO_2, H_2O, NO, NO_2
				23.5	23.5		ZnO

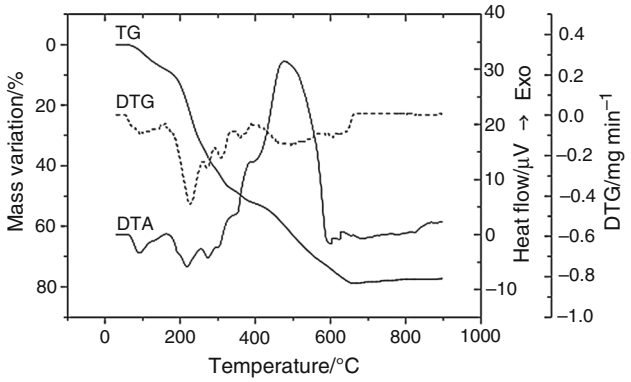

Fig. 4 TG, DTG and DTA curves of complex (**1**)

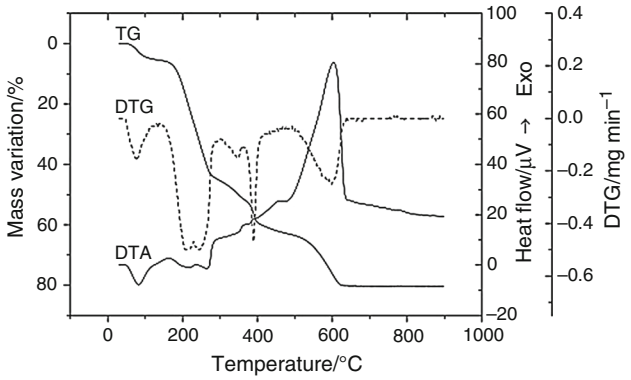

Fig. 5 TG, DTG and DTA curves of complex (**2**)

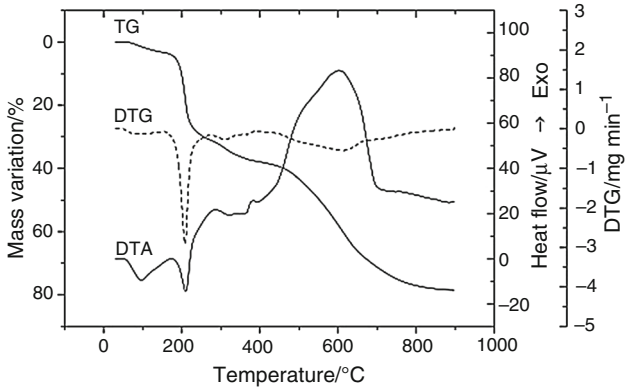

Fig. 6 TG, DTG and DTA curves of complex (**3**)

exothermic and endothermic overlapped processes. A CN fragment is eliminated from the organic matrix in the next step according with the mass loss and products as CO_2, H_2O, NO and the decomposition proceeds with oxidative degradation of the organic matrix. According with powder X-ray diffraction profile, the final product formed at 850 °C is CuO (ASTM 5-661) (found/calcd. overall mass loss: 78.6/78.1 %).

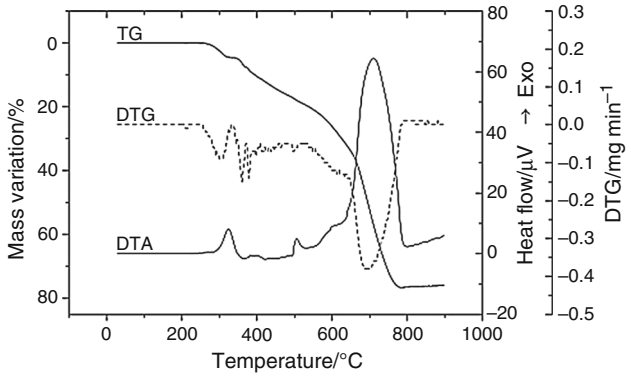

Fig. 7 TG, DTG and DTA curves of complex (**4**)

Compound (**4**) is anhydrous and as result its decomposition starts at 252 °C with methyl group elimination (Fig. 7). In the next step, the partial chloride anion elimination (75 %) proceeds according with the identified products in the gaseous mixture. This behaviour could be the result of chloride anion involving in different interactions in the compound network, besides coordinative ones. Fragments such as Cl, CO_2, HCO_2, H_2O, NO, NO_2 detected in the mass spectra of eliminated products indicate that in the third step several processes such as chloride elimination, bond cleavage, rearrangements and oxidative degradation occurs. As consequence, in the 544–787 °C range, two small exothermic events can be observed on the DTA curve profile. The residual mass at 787 °C corresponds to zinc (II) oxide (ASTM 036-1451) generations (found/calcd. overall mass loss: 76.1/76.5 %).

Taking into account all above data, complexes can be formulated as $[Co_2(pmtp)_2Cl_4(OH_2)_4]$ (**1**), $[Ni_2(pmtp)_2Cl_4(OH_2)_4]\cdot 2H_2O$ (**2**), $[Cu_2(pmtp)_2Cl_4(OH_2)_2]$ and $[Zn_2(pmtp)_2Cl_4]$, respectively (Scheme 1). For Zn(II) the tetrahedral stereochemistry was proposed having in view its anhydrous nature, the small number of ligands and its preference for this kind of surroundings in complexes with both large and negatively charged ligands such as chloride anion.

Antimicrobial activity against planktonic cells

The compound (**1**) exhibited good microbicidal activity against *E. coli, K. pneumoniae* reference strains, and MRSA (MIC of 125 μg mL^{-1}) and moderate activity against *B. subtilis* (MIC of 250 μg mL^{-1}). The compound (**2**) exhibited good antimicrobial activity against *B. subtilis* (MIC of 125 μg mL^{-1}) and moderate activity against *K. pneumoniae* 806 clinical strain and *P. aeruginosa* reference strain. Compound (**3**) exhibited very good activity against *B. subtilis* strain (MIC of 62.50 μg mL^{-1}) and moderate activity against a wide range of Gram-positive and Gram-

Table 4 The MIC values (μg mL^{-1}) for complexes (**1**)–(**4**)

Strain	(**1**)	(**2**)	(**3**)	(**4**)
E. coli ATCC 25922	125	500	250	62.50
E. coli 832	250	>1000	500	1000
K. pneumoniae ATCC 134202	125	>1000	250	62.50
K. pneumoniae 806	>1000	250	250	250
P. aeruginosa ATCC 27853	>1000	250	250	>1000
P. aeruginosa 392	>1000	500	500	500
S. aureus MRSA 1263	125	>1000	500	125
S. aureus ATCC 25923	>1000	>1000	250	62.50
B. subtilis ATCC 6633	250	125	62.50	62.50

Table 5 The complexes influence on biofilm formation (MBEC value, μg mL^{-1})

Strain	(**1**)	(**2**)	(**3**)	(**4**)
E. coli ATCC 25922	62.50	250	125	62.50
E. coli 832	62.50	–	250	–
K. pneumoniae ATCC 134202	62.50	–	62.50	31.25
K. pneumoniae 806	–	62.50	125	125
P. aeruginosa ATCC 27853	–	62.50	62.50	–
P. aeruginosa 392	–	125	125	250
S. aureus MRSA 1263	62.50	–	250	62.50
S. aureus ATCC 25923	–	–	62.50	31.25
B. subtilis ATCC 6633	125	62.50	31.25	31.25

negative strains including clinical resistant ones. Compound (**4**) proved to be most active, exhibiting low MIC values against *E. coli, K. pneumoniae, S. aureus* and *B. subtilis* reference strains, good activity against MRSA strains and moderate activity against *K. pneumoniae* clinical strain (Table 4).

It is worth to mention that a MIC value >500 μg mL^{-1} was considered as corresponding to a low, ≤500 to ≥250 μg mL^{-1} to moderate, <250 to ≥125 μg mL^{-1} to good and <125 μg mL^{-1} to a very good antimicrobial activity [53].

Antimicrobial activity against biofilm embedded cells

The tested compound exhibited a very good anti-biofilm activity at concentrations lower than the MIC value, demonstrating their potential to act as anti-pathogenic agents, which inhibit the expression of different virulence features (in the present case, the ability of bacterial strains to form biofilms on the inert substratum), without interfering with microbial growth. The advantages of anti-pathogenic versus microbicidal agents are the low probability of selecting resistance and the low risk of side effects caused by the high doses required for the occurrence of therapeutic action and by the induced dysbiosis of the normal microbiota [54].

For the compounds (**1**) and (**2**), the anti-biofilm microbial spectrum was similar to that of microbicidal one, including also the clinical *E. coli* and *P. aeruginosa* strains, but the MBEC values were two to four times lower than the MIC ones. The compound (**3**) exhibited moderate to very good anti-biofilm activity against all tested strains, the MBEC values being generally two times lower than the MIC values. For compound (**4**) the anti-biofilm spectrum was identical with the microbicidal one, by the MBEC values were in most cased two times lower than the MIC values (Table 5).

Conclusions

A new derivative 5-phenyl-7-methyl-1,2,4-triazolo[1,5-*a*]pyrimidine (pmtp) was synthesised and fully characterised by single crystal X-ray diffraction. Complexes of type $M(pmtp)Cl_2{\cdot}nH_2O$ (M: Co, Ni, Cu, Zn) with this ligand were synthesised and characterised through a wide range of physico-chemical methods.

The IR spectra of complexes exhibit the characteristic bands for triazolopyrimidine ring. Electronic spectra of Co(II) and Ni(II) complexes are characteristic for octahedral stereochemistry, while that of Cu(II) complex display the pattern of square pyramidal surrounding. These data were furthermore confirmed by magnetic behaviour at room temperature and EPR spectrum.

The thermal analyses evidenced processes as water and chloride anion elimination as well as fragmentation and oxidative degradation of the organic ligand. The formed gaseous products during decomposition were monitored by MS measurements. The final product of decomposition was metal (II) oxide, except for cobalt (II) complex where Co_3O_4 is formed. The results are in good agreement with the complexes composition.

Complexes exhibited moderate to very good antimicrobial activity against a wide spectrum of Gram-positive and Gram-negative bacterial strains, both reference and clinical resistant ones. The most effective compound proved to be (**4**) and (**3**), both against planktonic and biofilm cells. The minimal biofilm eradication values were two to four times lower than the minimal inhibitory concentrations demonstrating the potential of the obtained complexes to act as anti-pathogenic agents.

Acknowledgements The authors thank for EPR data to researcher Gabriela Ioniţă and for magnetic measurements at room temperature to researcher Nicolae Stanică, both from "Ilie Murgulescu" Physical Chemistry Institute of Romanian Academy.

References

1. Boechat N, Pinheiro LCS, Silva TS, Aguiar ACC, Carvalho AS, Bastos MM, Costa CCP, Pinheiro S, Pinto AC, Mendonça JS, Dutra KDB, Valverde AL, Santos-Filho OA, Ceravolo IP, Krettli AU. New trifluoromethyl triazolopyrimidines as anti-*Plasmodium falciparum* agents. Molecules. 2012;17:8285–302.
2. Said SA, Amr A-G, Sabry NM, Abdalla MM. Analgesic, anti-convulsant and anti-inflammatory activities of some synthesized benzodiazipine, triazolopyrimidine and bis-imide derivatives. Eur J Med Chem. 2009;44:4787–92.
3. Ashour HM, Shaaban OG, Rizk OH, El-Ashmawy IM. Synthesis and biological evaluation of thieno [2′,3′:4,5]pyrimido[1,2-b][1,2,4]triazines and thieno[2,3-d][1,2,4]triazolo[1,5-*a*]pyrimidines as anti-inflammatory and analgesic agents. Eur J Med Chem. 2013;62:341–51.
4. Yu W, Goddard C, Clearfield E, Mills C, Xiao T, Guo H. Design, synthesis, and biological evaluation of triazolo-pyrimidine derivatives as novel inhibitors of hepatitis B virus surface Antigen (HBsAg) secretion. J Med Chem. 2011;54:5660–70.
5. Zhang N, Ayral-Kaloustian S, Nguyen T, Afragola J, Hernandez R, Lucas J, Gibbons J, Beyer C. Synthesis and SAR of [1,2,4]triazolo[1,5-*a*]pyrimidines, a class of anticancer agents with a unique mechanism of tubulin inhibition. J Med Chem. 2007;50:319–27.
6. Beyer CF, Zhang N, Hernandez R, Vitale D, Lucas J, Nguyen T, Discafani C, Ayral-Kaloustian S, Gibbons JJ. TTI-237: a novel microtubule-active compound with in vivo antitumor activity. Cancer Res. 2008;68:2292–300.
7. Chen Q, Zhu XL, Jiang LL, Liu ZM, Yang GF. Synthesis, antifungal activity and CoMFA analysis of novel 1,2,4-triazolo[1,5-*a*]pyrimidine derivatives. Eur J Med Chem. 2008;43:595–603.
8. Novinson T, Springer RH, O'Brien DE, Scholten MB, Miller JP, Robins RK. 2-(Alkylthio)-1,2,4-triazolo[1,5-*a*]pyrimidines as adenosine cyclic 3′,5′-monophosphate phosphodiesterase inhibitors with potential as new cardiovascular agents. J Med Chem. 1982;25:420–6.
9. El-Gendy MMA, Shaaban M, Shaaban KA, El-Bondkly AM, Laatsch H. Essramycin: a first triazolopyrimidine antibiotic isolated from nature. J Antibiot. 2008;61:149–57.
10. Ohnishi H, Yamaguchi K, Shimada S, Suzuki Y, Kumagai A. A new approach to the treatment of atherosclerosis and trapidil as an antagonist to platelet-derived growth factor. Life Sci. 1981;28:1641–6.
11. Salas JM, Quirós M, Haj MA, Magán R, Marin C, Sánchez-Moreno M, Faure R. Activity of Pt(II) and Ru(III) triazolopyrimidine complexes against parasites of the genus *Leishmania,* Trypanosomas and Phytomonas. Metal Based Drugs. 2001;8:119–24.
12. Ramírez-Macías I, Marín C, Salas JM, Caballero A, Rosales MJ, Villegas N, Rodríguez-Dieguez A, Barea E, Sánchez-Moreno M. Biological activity of three novel complexes with the ligand 5-methyl-1,2,4-triazolo[1,5-*a*]pyrimidin-7(4H)-one against *Leishmania* spp. J Antimicrob Chemother. 2011;66:813–9.
13. Ramírez-Macías I, Maldonado CR, Marín C, Olmo F, Gutiérrez-Sánchez R, Rosales MJ, Quirós M, Salas JM, Sánchez-Moreno M. In vitro anti-leishmania evaluation of nickel complexes with a triazolopyrimidine derivative against *Leishmania infantum* and *Leishmania braziliensis*. J Inorg Biochem. 2012;112:1–9.
14. Tahghighi A. Importance of metal complexes for development of potential leishmanicidal agents. J Organomet Chem. 2014;770:51–60.
15. Caballero AB, Rodríguez-Diéguez A, Quirós M, Salas JM, Huertas Ó, Ramírez-Macías I, Olmo F, Marín C, Chaves-Lemaur G, Gutierrez-Sánchez R, Sánchez-Moreno M. Triazolopyrimidine compounds containing first-row transition metals and their activity against the neglected infectious Chagas disease and leishmaniasis. Eur J Med Chem. 2014;85:526–34.
16. Caballero AB, Rodríguez-Diéguez A, Salas JM, Sánchez-Moreno M, Marín C, Ramírez-Macías I, Santamaría-Díaz N, Gutiérrez-Sánchez R. Lanthanide complexes containing 5-methyl-1,2,4-triazolo[1,5-*a*]pyrimidin-7(4H)-one and their therapeutic potential to fight leishmaniasis and Chagas disease. J Inorg Biochem. 2014;138:39–46.
17. Caballero AB, Marín C, Rodríguez-Diéguez A, Ramírez-Macías I, Barea E, Sánchez-Moreno M, Salas JM. *In vitro* and in vivo antiparasital activity against *Trypanosoma cruzi* of three novel 5-methyl-1,2,4-triazolo[1,5-*a*]pyrimidin-7(4H)-one-based complexes. J Inorg Biochem. 2011;105:770–6.
18. Bavelaar K, Khalil R, Mutikainen I, Turpeinen U, Marquès-Gallego P, Kraaijkamp M, van Albada GA, Haasnoot JG, Reedijk J. A dinuclear silver compound with 5,6,7-trimethyl-[1,2,4]triazolo[1,5-*a*]pyrimidine with a short Ag-Ag bond. Synthesis, characterization, single-crystal structure analysis and cytostatic activity. Inorg Chim Acta. 2011;366:81–4.
19. Ruiz J, Villa MD, Cutillas N, López G, de Haro C, Bautista D, Moreno V, Valencia L. Palladium(II) and platinum(II) organometallic complexes with 4,7-dihydro-5-methyl-7-oxo[1,2,4]-triazolo[1,5-*a*]pyrimidine. Antitumor activity of the platinum compounds. Inorg Chem. 2008;47:4490–505.
20. Łakomska I, Wojtczak A, Sitkowski J, Kozerski L, Szłyk E. Platinum(IV) complexes with purine anolgs. Studies of molecular structure and proliferative activity in vitro. Polyhedron. 2008;27:2765–70.
21. Łakomska I, Kooijman H, Spek AL, Shen WZ, Reedijk J. Mono- and dinuclear platinum(II) compounds with 5,7-dimethyl-1,2,4-triazolo[1,5-*a*]pyrimidine. Structure, cytotoxic activity and reaction with 5′-GMP. Dalton Trans. 2009;48:10736–41.
22. Łakomska I, Fandzloch M, Wojtczak A, Szłyk E. Platinum(IV) coordination compounds containing 5-methyl-1,2,4-triazolo[1,5-*a*]pyrimidin-7(4H)-one as nonleaving ligand. Molecular and cytotoxicity in vitro characterization. Spectrochim Acta A Mol Biomol Spectrosc. 2011;79:497–501.
23. Łakomska I, Hoffmann K, Topolski A, Kloskowski T, Drewa T. Spectroscopic, kinetic and cytotoxic in vitro study of hexafluoroglutarate platinum(II) complex with 5,7-dimethyl-1,2,4-triazolo[1,5-*a*]pyrimidine. Inorg Chim Acta. 2012;387:455–9.
24. Łakomska I, Fandzloch M, Muzioł T, Sitkowski J, Wietrzyk J. Structure-cytotoxicity relationship for different types of mononuclear platinum(II) complexes with 5,7-ditertbutyl-1,2,4-triazolo[1,5-*a*]pyrimidine. J Inorg Biochem. 2012;115:100–5.
25. Łakomska I, Fandzloch M, Muzioł T, Lis T, Jezierska J. Synthesis, characterization and antitumor properties of two highly cytotoxic ruthenium(III) complexes with bulky triazolopyrimidine ligands. Dalton Trans. 2013;42:6219–26.
26. Łakomska I, Fandzloch M, Wojtczak A. Dimeric ruthenium-triazolopyrimidine complex: synthesis and structural characterization. Inorg Chem Commun. 2014;49:24–6.
27. Fandzloch M, Wojtczak A, Sitkowski J, Łakomska I. Interaction of ruthenium(II) and ruthenium(III) ions with 5-methyl-1,2,4-triazolo[1,5-*a*]pyrimidin-7(4H)-one. Polyhedron. 2014;67:410–5.
28. Hoffmann K, Łakomska I, Wiśniewska J, Kaczmarek-Kędziera A, Wietrzyk J. Acetate platinum(II) compound with 5,7-ditert-butyl-1,2,4-triazolo[1,5-*a*]pyrimidine that overcomes cisplatin resistance: structural characterization, in vitro cytotoxicity, and kinetic studies. J Coord Chem. 2015;68:3193–208.
29. Girasolo MA, Attanzio A, Sabatino P, Tesoriere L, Rubino S, Stocco G. Organotin(IV) derivatives with 5,7-disubstituted-1,2,4-triazolo[1,5-*a*]pyrimidine and their cytotoxic activities: the importance of being conformers. Inorg Chim Acta. 2014;423:168–76.
30. Romero MA, Salas JM, Quirós M. Cobalt(II) complexes of 5,7-dimethyl[1,2,4]-triazolo-[1,5-*a*]-pyrimidine. Spectroscopic characterization, XRD study and antimicrobial activity. Trans Met Chem. 1993;18:595–8.

31. Girasolo MA, Salvo CD, Schillaci D, Barone G, Silvestri A, Ruisi G. Synthesis, characterization, and in vitro antimicrobial activity of organotin(IV) complexes with triazolo-pyrimidine ligands containing exocyclic oxygen atoms. J Organomet Chem. 2005;690:4773–83.
32. Girasolo MA, Schillaci D, Di Salvo C, Barone G, Silvestri A, Ruisi G. Synthesis, spectroscopic characterization and in vitro antimicrobial activity of diorganotin(IV) dichloride adducts with [1,2,4]triazolo-[1,5-*a*]pyrimidine and 5,7-dimethyl-[1,2,4]triazolo[1,5-a]pyrimidine. J Organomet Chem. 2006;691:693–701.
33. Ruisi G, Canfora L, Bruno G, Rotondo A, Mastropietro TF, Debbia EA, Girasolo MA, Megna B. Triorganotin(IV) derivates of 7-amino-2-(methylthio)[1,2,4]triazolo[1,5-*a*]pyrimidine-6-carboxylic acid. Synthesis, spectroscopic characterization, in vitro antimicrobial activity and X-ray crystallography. J Organomet Chem. 2010;695:546–51.
34. Girasolo MA, Canfora L, Sabatino P, Schillaci D, Foresti E, Rubino S, Ruisi G, Stocco G. Synthesis, characterization, crystal structures and *in vitro* antistaphylococcal activity of organotin(IV) derivatives with 5,7-disubstituted-1,2,4-triazolo[1,5-*a*]pyrimidine. J Inorg Biochem. 2012;106:156–63.
35. Abul-Haj M, Quirós M, Salas JM. Divalent transition metal complexes of the anionic form of 4,7-dihydro-1,2,4-triazolo[1,5-*a*]pyrimidine-7-one: crystal structure of the zinc(II) compound. Polyhedron. 2004;23:743–7.
36. Hooft RWW. Bruker AXS, Delft, The Netherlands, 2008.
37. Otwinowski Z, Minor W. Processing of X-ray diffraction data collected in oscillation mode. Meth Enzymol. 1997;276:307–26.
38. Otwinowski Z, Borek D, Majewski W, Minor W. Multiparametric scaling of diffraction intensities. Acta Crystallogr A. 2003;59:228–34.
39. Sheldrick GM. Phase annealing in SHELX-90: direct methods for larger structures. Acta Crystallogr A. 1990;4:467–73.
40. Sheldrick GM. A short history of SHELX. Acta Crystallogr A. 2008;6:112–22.
41. BrukerAXS, 2000.
42. Calu L, Badea M, Chifiriuc MC, Bleotu C, David G-I, Ioniţă C, Măruţescu L, Lazăr V, Stanică N, Irina Soponaru I, Dana Marinescu D, Olar R. Synthesis, spectral, thermal, magnetic and biological characterization of Co(II), Ni(II), Cu(II) and Zn(II) complexes with a Schiff base bearing a 1,2,4-triazole pharmacophore. J Therm Anal Calorim. 2015;120:375–86.
43. Geary WJ. The use of conductivity measurements in organic solvents for the characterisation of coordination compounds. Coord Chem Rev. 1971;7:81–122.
44. Odabasoglu M, Büyükgüngör O. 5,7-Dimethyl-1,2,4-triazolo[1,5-*a*]pyrimidine. Acta Cryst. 2006;E62:o1310–1.
45. Nakamoto K (2009) Infrared and Raman Spectra of Inorganic and Coordination Compounds, 6th ed., Part B. Applications in Coordination, Organometallic, and Bioinorganic Chemistry. New Jersey: Wiley.
46. Solomon EI, Lever ABP, Inorganic Electronic Structure and Spectroscopy, Vol. II, Applications and Case Studies, New York, Chichester, Weinheim, Brisbane, Singapore, Toronto: John Wiley & Sons; 2006.
47. König E. The Nephelauxetic Effect. Calculation and Accuracy of the Interelectronic Repulsion Parameters I. Cubic High-Spin d^2, d^3, d^7 and d^8 Systems. Struct Bound. 1972;9:175-372.
48. Gispert JR. Coordination Chemistry. Weinheim: Wiley-VCH; 2008.
49. Hathaway BJ, Billing DE. The electronic properties and stereochemistry of mono-nuclear complexes of the copper(II) ion. Coord Chem Rev. 1970;5:143–207.
50. El Metwally NM, Arafa R, El-Ayaan U. Molecular modeling, spectral, and biological studies of 4-formylpyridine-4 N-(2-pyridyl) thiosemicarbazone (HFPTS) and its Mn(II), Fe(III), Co(II), Ni(II), Cu(II), Cd(II), Hg(II), and UO_2(II) complexes. J Therm Anal Calorim. 2014;115:2357–67.
51. Abdel-Kader NS, Amin RM, El-Ansary AL. Complexes of Schiff base of benzopyran-4-one derivative. Synthesis, characterization, non-isothermal decomposition kinetics and cytotoxicity studies. J Therm Anal Calorim. 2016; 123:1695-706.
52. Lalia-Kantouri M, Parinos K, Gdaniec M, Chrissafis K, Ferenc W, Papadopoulos CD, Czapik A, Sarzynski J. Thermoanalytical, magnetic and structural investigation of Co(II) complexes with dipyridylamine and 2-hydroxyphenones. J Therm Anal Calorim. 2014;116:249–58.
53. Limban C, Chifiriuc MC. Antibacterial Activity of New Dibenzoxepinone Oximes with Fluorine and Trifluoromethyl Group Substituents. Int J Mol Sci. 2011;12:6432–44.
54. Patrinoiu G, Calderón-Moreno JM, Chifiriuc CM, Saviuc C, Birjega R, Carp O. Tunable ZnO spheres with high anti-biofilm and antibacterial activity via a simple green hydrothermal route. J Colloid Interface Sci. 2016;462:64–74.